Correlation between Critical Temperature and Strength of Small-Scale bcc Pillars

A. S. Schneider,[1] D. Kaufmann,[2] B. G. Clark,[1,3,*] C. P. Frick,[4] P. A. Gruber,[5] R. Mönig,[2] O. Kraft,[2,5] and E. Arzt[3,6,†]

[1]*Max Planck Institute for Metals Research, Heisenbergstrasse 3, 70569 Stuttgart, Germany*
[2]*Forschungszentrum Karlsruhe, Institut für Materialforschung II, Hermann-von-Helmholtz-Platz 1, 76344 Eggenstein-Leopoldshafen, Germany*
[3]*INM-Leibniz Institute for New Materials, Campus Building D2 2, 66123 Saarbrücken, Germany*
[4]*Mechanical Engineering Department, University of Wyoming, 1000 East University Avenue, Laramie, Wyoming 82071, USA*
[5]*Institut für Zuverlässigkeit von Bauteilen und Systemen, Universität Karlsruhe, Kaiserstrasse 12, 76131 Karlsruhe, Germany*
[6]*Saarland University, 66123 Saarbrücken, Germany*

(Received 4 May 2009; published 31 August 2009)

Microcompression tests were performed on focused-ion-beam-machined micropillars of several body-centered-cubic metals (W, Mo, Ta, and Nb) at room temperature. The relationship between yield strength and pillar diameter as well as the deformation morphologies were found to correlate with a parameter specific for bcc metals, i.e., the critical temperature T_c. This finding sheds new light on the phenomenon of small-scale plasticity in largely unexplored non-fcc metals.

DOI: 10.1103/PhysRevLett.103.105501 PACS numbers: 62.25.−g

Recent experiments involving compression of small-scale pillars formed by focused-ion-beam (FIB) micromachining have shown that the size dependence of the yield stress differs fundamentally between face-centered-cubic (fcc) and body-centered-cubic (bcc) metals. In both materials, the yield strength σ_y scales inversely with some power of the pillar diameter d: In fcc pillars the relationship is $\sigma_y \propto d^{-0.6}$–$d^{-1.0}$ [1–5], whereas bcc pillars exhibit a less pronounced size effect with $\sigma_y \propto d^{-0.22}$–$d^{-0.45}$ [6,7]. Various models including size-dependent dislocation nucleation [8,9] and dislocation starvation [10] have been proposed to account for size effects in fcc metals. In bcc metals, dislocation processes differ from those in fcc crystals: Dislocation motion occurs on various slip systems with screw dislocations being slower than edge dislocations. The low mobility of screw dislocations is due to their nonplanar core structure and the associated need to overcome the Peierls potential by thermal activation [11,12]. The different size dependence for bcc pillars has been attributed to the low mobility of screw dislocations leading to enhanced dislocation-dislocation interactions [13] or to kinetic pileups of screw dislocations in the vicinity of dislocation sources [7].

In this study, compression experiments were conducted at room temperature on bcc metals with different critical temperatures (Table I) to investigate the effect of screw dislocation mobility on the size effect of bcc pillars. The critical temperature (T_c) is defined as the temperature at which the flow stress becomes insensitive to the test temperature; i.e., screw and edge dislocations have equal mobility due to thermal activation of the screw dislocations [18]. Below T_c, screw dislocations are less mobile than edge dislocations, and their mobility is a function of test temperature T_{test} relative to T_c.

Tungsten, molybdenum, and niobium [001]-oriented samples were cut from high purity single crystals grown by the Czochralski method by electron discharge machining. The crystallographic orientation of the samples was determined before cutting by Laue diffraction. Tantalum pillars were cut in [001]-oriented grains of a polycrystal after electron backscatter diffraction mapping of the sample surface. For all materials, pillars with diameters ranging from 200 nm to 6 μm, an approximate aspect ratio of 3:1, and taper angles of roughly 3° were machined with a FIB (Dual Beam™ FIB) on the surfaces of the [001]-oriented samples. In total, 155 pillars were compressed under load control with a 10 μm sapphire or diamond flat punch using a nanoindenter device (MTS XP). In order to minimize the effects of variation in strain rate, the load rate was scaled with the cross-sectional area of the pillars resulting in comparable stress rates for all pillars of 33 ± 23 MPa/s. For consistency, the diameter measured at the top of the pillar was used to calculate the engineering stress-strain relationship. A detailed description of fabrication, testing, and analysis can be found in Ref. [5].

Representative compressive stress-strain curves for [001]-oriented W, Mo, Ta, and Nb pillars for various diameters are shown in Fig. 1. The overall shapes of the stress-strain curves are typical for load-controlled single crystal pillar compression and display the stochastic nature of slip in small dimensions. Strength increases markedly with decreasing diameter. The shape of the stress-strain curve for pillars larger than roughly 2 μm resembles bulk

TABLE I. Critical temperatures of the bcc metals used in this study; data from Refs. [14–17]. $T_{\text{test}} = 298$ K in our experiments.

Material	Nb	Ta	Mo	W
Critical temperature T_c (K)	350	450	480	800
Temperature ratio T_{test}/T_c	0.85	0.66	0.62	0.37

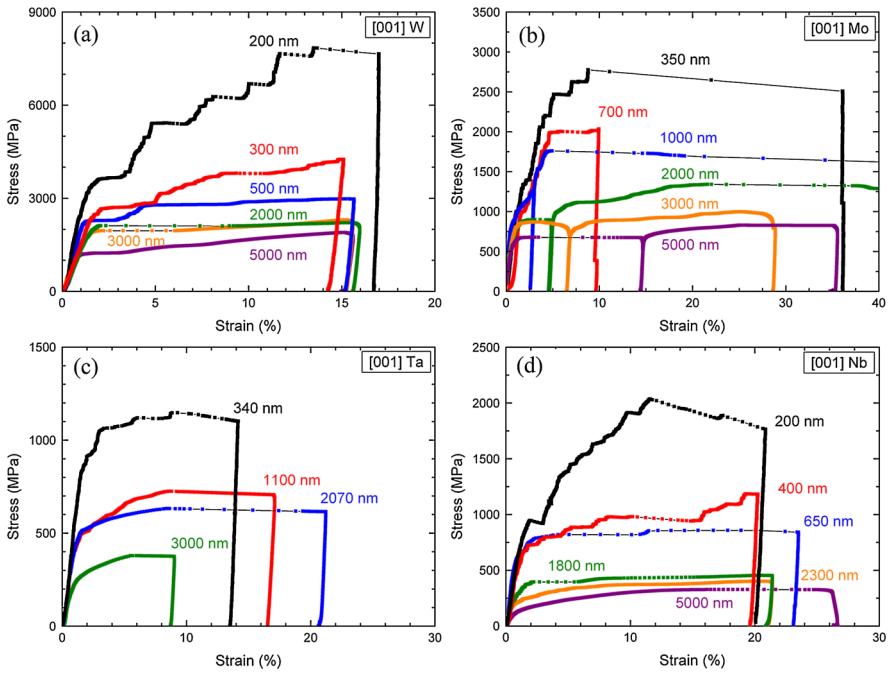

FIG. 1 (color online). Representative stress-strain curves for [001] (a) W, (b) Mo, (c) Ta, and (d) Nb pillars over a range of diameters from 200 nm to 6 μm. Details about (b) can be found in Ref. [7].

flow [14–17] with a gradual transition from elastic to plastic deformation and relatively little strain hardening. Pillars with smaller diameters exhibit strain bursts associated with individual dislocation events [19]. In general, increasing strain hardening was observed with decreasing diameter, with the exception of large strain bursts in small pillars that led to an apparent strain softening. Increasing strain hardening rates can be explained in terms of kinetic hardening [7]. Although the nominal values for the materials tested are different, the qualitative features of the stress-strain response are consistent with one another and are similar to observations in fcc single crystalline pillars [4]. The stress-strain response was analyzed in a previous study [20], showing that the distribution of strain bursts in bcc Mo for a given diameter was remarkably similar to that of fcc pillars.

Figure 2 shows representative scanning electron microscope (SEM) images of deformed W and Nb pillars with diameters close to 200 nm [Figs. 2(a) and 2(b)] and 5 μm [Figs. 2(c) and 2(d)]. Pictures of Mo [7] and Ta [21] pillars are not shown in the interest of space; however, the deformation morphology of Mo is similar to that of W and the behavior of Ta coincides with that of Nb. All pillars show traces indicative of multiple slip. Pillars with diameters smaller than approximately 1–2 μm exhibited localized slip on a few glide planes, preferentially at the top, as shown in Figs. 2(a) and 2(b). For pillars with larger diameters, two different deformation morphologies were identified. In large W and Mo pillars, there are no continuous slip steps on the pillar surfaces. The slip steps appear wavy throughout the sample, as is typically observed for bulk bcc metals [11,18]. Wavy slip planes are consistently more difficult to observe in the Ta and Nb pillars, which primarily exhibit localized slip on preferred glide planes with clear slip traces ranging across the pillar surface. The deformation morphology for Nb is in agreement with experimental findings by Kim, Jang, and Greer [22].

The mechanical size effect of different bcc pillars is shown in Fig. 3(a), which illustrates the stress at 5% strain as a function of diameter. The data for Mo from a recent study by Brinckmann, Kim, and Greer [6] are consistent with the presented Mo data, as shown in Ref. [7]. For comparison, typical fcc data from Au pillars with low symmetry compression axes [4] were added. The strengths of the bcc metals are higher than those of Au, and the relative differences in strength between the different materials decrease with decreasing pillar size. Comparing W and Nb, the strengths differ by a factor of 5.5 at 5 μm (1410 vs 257 MPa) and differ only by a factor of 2.2 at 200 nm (2800 vs 1275 MPa). The order of the strength of the bcc pillars correlates with the critical temperature of the individual material. By using a power law fit, slopes of -0.21, -0.38, -0.41, and -0.48 are obtained for W, Mo, Ta, and Nb pillars, respectively. The slope for the Nb pillars is significantly smaller than recently observed by Kim, Jang, and Greer [22]. This difference is most likely a reflection of the stochastic nature of the stress-strain response of small-scale pillars in combination with the limited number of tests performed in the study by Kim, Jang, and Greer [22]. By comparing the slopes of the current study with the critical temperatures given in Table I, it can be seen that the higher the critical temperature, the weaker the size dependence. It is important to note that this trend is independent of the strain value at which the stresses are measured or of specific normalization conditions [21]. In Fig. 3(b), the power law exponent is plotted as a function of test temperature divided by T_c, to examine the role of screw dislocation mobility on the size dependence. The

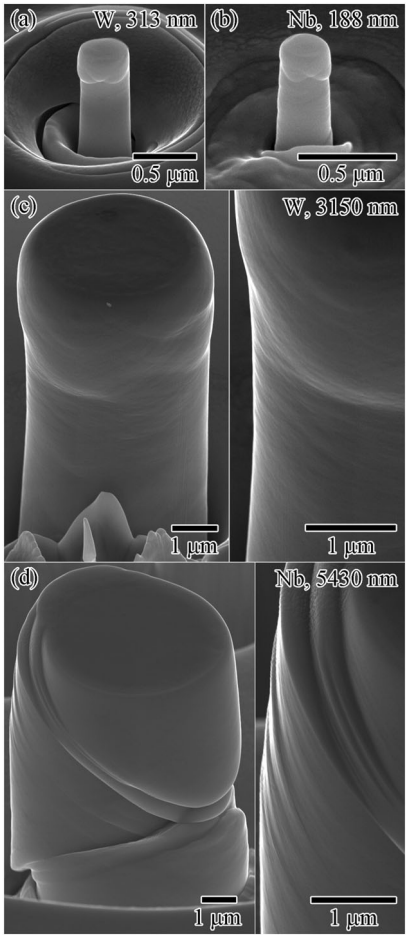

FIG. 2. Postcompression SEM images of representative [001]-oriented Nb and W pillars: (a) 313 nm W, (b) 188 nm Nb, (c) 4870 nm W, and (d) 5430 nm Nb pillars. Higher magnification insets in (c) and (d) highlight differences in slip trace morphologies between W and Nb. In all cases, slip traces on the pillar surfaces indicate multiple slip.

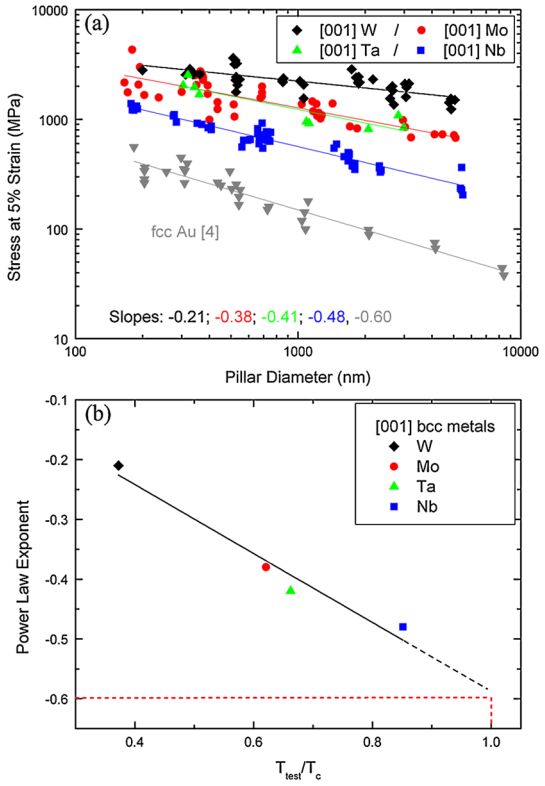

FIG. 3 (color online). Comparison plots: (a) of stress measured at 5% strain versus pillar top diameter for all [001] bcc pillars tested (i.e., W, Mo, Ta, and Nb) as well as [001] Au pillar data [4]; (b) slope of the line of best fit (exponent) for the size dependence of the bcc metals shown in (a) versus normalized test temperature T_{test}/T_c (see text and Table I).

ratio of T_{test} to T_c is a measure for the thermal activation of the screw dislocations: A larger ratio means higher thermal activation and therefore higher mobility of the screw dislocations. The data points in Fig. 3(b) follow roughly a linear relationship. The extrapolation of the line of best fit to lower critical temperatures yields an exponent of about -0.6 [represented by the horizontal line in Fig. 3(b)] for $T_c = T_{\text{test}}$, which corresponds to the condition where screw and edge dislocations have equal mobility. This value is in agreement with exponents found for fcc metal pillars [3,4], where screw and edge dislocations have the same mobility at room temperature.

The results presented here show that deformation mechanisms in small-scale bcc metals depend on size as well as on critical temperature. All materials tested show an increase in strength with decreasing pillar diameter, indicating that confinement of dislocation processes starts to dominate the deformation; this leads to a transition from continuous to jerky stress-strain behavior and a significant change in the deformation morphology between small and large pillars. The critical temperature of the bcc metals was found to have a strong influence on the deformation morphology of the large pillars. Large pillars with low T_c (Ta, Nb) showed localized slip, whereas metals with higher T_c (Mo, W) show wavy slip as is typically observed for bulk bcc metals [Figs. 2(c) and 2(d)]. In general, the deformation of bcc metals is controlled by the motion of long and straight screw dislocations [11]. Their ability to cross-slip between crystallographic planes which intersect along the $\langle 111 \rangle$ direction leads to wavy slip steps. The cross-slip of screw dislocations may account for the deformation morphology of the large W and Mo pillars. The well-resolved slip steps of Nb and Ta indicate that less cross-slip occurred during deformation. For metals with low T_c (Nb, Ta), the dislocations may bow out and deviate from pure screw character over a considerable length of the pillar. As dislocations of mixed character are confined to specific glide planes, this may lead to localized slip. For small pillars, no influence of the critical temperature on deformation morphology was found. One explanation is that the periodicity of wavy slip is on the order of the pillar diameter and hence not observable at this size scale. Another possible explanation is that for the smallest pillars dislocation nucleation is controlling the deformation instead of dislocation propagation. Immediately after nucleation, dislocations are

highly curved and therefore of mixed character, explaining the localized deformation of the smallest pillars [Figs. 2(a) and 2(b)]. This indicates that thermally activated screw dislocation motion and related processes are not prevalent in very small bcc pillars. However, in a previous study on Mo pillars [7] it was shown that the strain rate dependence of the yield strength does not depend on pillar diameter and that it is comparable to values obtained from bulk materials. This suggests that, on the one hand, athermal dislocation nucleation controls the deformation at small size scales but a thermal component still exists. This is in contrast to nanocrystalline bcc metals, where it was found that the strain rate sensitivity decreases with decreasing grain size [23]. This indicates that at a small scale the interaction of dislocations with interfaces becomes dominant rather than screw dislocation motion as such.

Besides the deformation morphologies, the strength values and their size dependence were also found to correlate with T_c (Fig. 3). A general correlation of the strength values with T_c is not surprising as the strength of bcc bulk metals at temperatures below T_c is related to the low mobility of screw dislocations. As T_c increases from Nb to W, the mobility of screw dislocations decreases because thermal energy becomes small relative to the height of the Peierls potential, resulting in high stresses for materials with a high T_c. The correlation between size dependence and T_c suggests that the mobility of screw dislocations affects the size scaling: (i) From Fig. 3(a), it can be seen that, for the pillars with the smallest diameters, the relative differences in strength between the different materials are smallest, suggesting that the relative contribution of the Peierls mechanism on the overall strength decreases for decreasing sample size. (ii) As can be seen in Fig. 3(b), the power law exponent scales with the inverse of the critical temperature. It seems that for temperatures close to T_c, where the influence of the low mobility of screw dislocations becomes negligible, the behavior of bcc also approaches that of fcc metals. The similar behavior of fcc and bcc pillars for small diameters and for test temperatures near T_c indicates that, under conditions where screw dislocation motion is not the limiting mechanism, the strength of bcc and fcc pillars may be controlled by the same dislocation processes. With increasing sample size and increasing critical temperature, an increasing effect of screw dislocation mobility becomes apparent, leading to a deviation from fcc behavior that scales with T_{test}/T_c.

One concept that can account for observations (i) and (ii) is based on kink nucleation at the sample surface [21,24]. Kinks can easily nucleate at the sample surface and can enhance screw dislocation mobility. Since the surface to volume ratio increases with decreasing sample size, kink nucleation becomes more likely and the mobility of screw dislocations may increase, possibly reaching the mobility of edge dislocations for the smallest samples. Another mechanism that can account for both observations (i) and (ii) is the kinetic pileup of screw dislocations in front of dislocation sources [7,25] which exert a back stress on the source. In smaller bcc pillars, only small pileups can form and less back stress is exerted on the dislocation source so that the activation stress is more or less determined by the line tension of the emitted dislocation. The influence of both mechanisms depends on the mobility of screw dislocations indicating that the critical temperature appears as an additional parameter influencing the deformation behavior of bcc metals in small dimensions.

The authors thank Arnold Weible and Christof Schwenk for sample preparation and Dan Gianola for fruitful discussions. B. G. C. thanks the Alexander von Humboldt Foundation for financial support. D. K., R. M., and O. K. acknowledge support by the European Union through the NANOMESO project.

*Present address: Sandia National Laboratories, Albuquerque, NM 87185, USA.
†Corresponding author.
Eduard.Arzt@inm-gmbh.de

[1] M. D. Uchic *et al.*, Science **305**, 986 (2004).
[2] J. R. Greer, W. C. Oliver, and W. D. Nix, Acta Mater. **53**, 1821 (2005).
[3] D. M. Dimiduk, M. D. Uchic, and T. A. Parthasarathy, Acta Mater. **53**, 4065 (2005).
[4] C. A. Volkert and E. T. Lilleodden, Philos. Mag. **86**, 5567 (2006).
[5] C. P. Frick *et al.*, Mater. Sci. Eng. A **489**, 319 (2008).
[6] S. Brinckmann, J.-Y. Kim, and J. R. Greer, Phys. Rev. Lett. **100**, 155502 (2008).
[7] A. S. Schneider *et al.*, Mater. Sci. Eng. A **508**, 241 (2009).
[8] T. A. Parthasarathy *et al.*, Scr. Mater. **56**, 313 (2007).
[9] S. I. Rao *et al.*, Philos. Mag. **87**, 4777 (2007).
[10] J. R. Greer and W. D. Nix, Phys. Rev. B **73**, 245410 (2006).
[11] J. W. Christian, Metall. Trans. A **14**, 1237 (1983).
[12] A. Seeger, Z. Metallkd. **93**, 760 (2002).
[13] J. R. Greer, C. R. Weinberger, and W. Cai, Mater. Sci. Eng. A **493**, 21 (2008).
[14] A. Seeger and U. Holzwarth, Philos. Mag. **86**, 3861 (2006).
[15] M. Werner, Phys. Status Solidi A **104**, 63 (1987).
[16] L. Hollang, M. Hommel, and A. Seeger, Phys. Status Solidi A **160**, 329 (1997).
[17] D. Brunner and V. Glebovsky, Mater. Lett. **42**, 290 (2000).
[18] B. Sestak and A. Seeger, Z. Metallkd. **69**, 195 (1978).
[19] D. M. Dimiduk *et al.*, Science **312**, 1188 (2006).
[20] M. Zaiser *et al.*, Philos. Mag. **88**, 3861 (2008).
[21] D. Kaufmann, R. Mönig, C. A. Volkert, and O. Kraft, Int. J. Plast. (to be published).
[22] J. Y. Kim, D. Jang, and J. R. Greer, Scr. Mater. **61**, 300 (2009).
[23] Q. Wei *et al.*, Mater. Sci. Eng. A **381**, 71 (2004).
[24] C. R. Weinberger and W. Cai, Proc. Natl. Acad. Sci. U.S.A. **105**, 14 304 (2008).
[25] R. Gröger and V. Vitek, Philos. Mag. Lett. **87**, 113 (2007).